

NON-HOMOGENEOUS EFFECTS ON SPATIOTEMPORAL CHAOS IN COUPLED LOGISTIC MAPS

Andre Varella Guedes, andre_varella@yahoo.com.br

Marcelo Amorim Savi, savi@mecanica.ufrj.br

Universidade Federal do Rio de Janeiro

COPPE – Department of Mechanical Engineering

21.941.972 – Rio de Janeiro – RJ, Brazil, P.O. Box 68.503

Abstract. Spatiotemporal characteristics of a dynamical system are one of the important aspects related to the complexity of natural systems. This research effort deals with the spatiotemporal dynamics of coupled logistic maps. The logistic map lattice is coupled from a power law. Non-homogeneous behaviors of the grid are of concern evaluating the spatial interaction of different kinds of behaviors. Basically, the grid is split in two parts where each one can present qualitative different responses when isolated. Under this condition, the global dynamics is investigated evaluating how both parts interact to each other. Periodic boundary conditions are analyzed assuming that the values of the maps are repeated for every N maps. The influence of initial conditions is also of concern. Results show situations involving periodic and chaotic patterns.

Keywords: Chaos, logistic maps, Lyapunov exponent, entropy, complexity, pattern formation.

1. INTRODUCTION

Complexity is a term that is being used to denote the main characteristics of complex systems. In general, complexity of natural systems has characteristics such as self-organization and adaptive abilities that leads to pattern formation. Order and chaos are both related to this complexity and the balance between them occurs in the edge of chaos where “life has enough stability to sustain itself and enough creativity to be named as life” (Waldrop, 1992). The edge of chaos defines a region of spontaneity that is proper to life. Spatiotemporal characteristic of a dynamical system is one of the important aspects related to the complexity of natural systems.

Literature presents numerous investigations concerning coupled maps. The key motivation is the search for universal properties and behaviors that apply to all dynamical systems. Therefore, coupled maps could be understood as prototypes of high dimensional dynamical systems. In general, synchronization of spatiotemporal dynamics is most intensively studied and there is a lack concerning the systematic investigation of other aspects of the system dynamics (Chazottes & Fernandes, 2005). In this regard, it is important to evaluate other aspects related to spatiotemporal dynamics.

This article deals with the spatiotemporal dynamics of coupled maps. These maps represent a mathematical idealization of physical systems that are discrete in time and space and have been used to describe the evolution and pattern formation in different systems as chemical reactions, turbulence, neural networks and population dynamics. Specifically, this work is focused on a system composed by coupled logistic maps where coupling is described by a power law. Therefore, each map has the influence of other maps from its neighborhood and boundary conditions are also important to define the coupling characteristics. Periodic boundary conditions where the values of the maps are repeated for every N maps is of concern. The comparison between responses is made by the observation of the dynamics and the values of the Kolmogorov-Sinai entropy density. The influence of initial conditions is also treated.

Non-homogeneous behaviors of the grid are of concern evaluating the spatial interaction of different kinds of behaviors. Basically, the grid is split in two parts where each one can present qualitative different responses when isolated. Under this condition, the global dynamics is investigated evaluating how both parts interact to each other. Numerical simulations allow one to conclude what types of conditions present greater tendency to develop chaotic, periodic and synchronized responses.

2. COUPLED MAPS

The logistic map is employed to describe different problems related to economic and social areas. The logistic map is a first order difference equation represented by: $x_{n+1} = f(x_n; \beta) = \beta x_n (1 - x_n)$. Recently, coupled logistic maps are being used in order to model the evolution and pattern formation in systems associated with chemical reactions, turbulence, neural networks and population dynamics (Holden & Zhang, 1992).

This work used a grid of N logistic maps where coupling is described by a power law as follows (Viana *et al.*, 2005):

$$x_{n+1}^{(i)} = (1 - \varepsilon) f(x_n^{(i)}) + \frac{\varepsilon}{\eta(\alpha)} \sum_{j=1}^{N'} \frac{1}{j^\alpha} [f(x_n^{(i+j)}) + f(x_n^{(i-j)})] \quad (1)$$

where $N=(N-1)/2$ and $f(x) = \beta x(1-x)$; ε is the coupling intensity ($0 \leq \varepsilon \leq 1$), α is the coupling coverage ($\alpha \geq 0$), and η is given by:

$$\eta(\alpha) = 2 \sum_{j=1}^{N'} j^{-\alpha} \tag{2}$$

Each map i depends of its neighbors and the boundary conditions define the maps when $i > N$ e $i < 1$. Figure 1 represents the coupled maps grid, illustrating the boundaries.

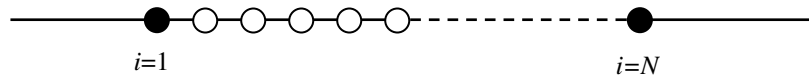


Figure 1. Coupled map grid.

A numerous of boundary conditions can be established in order to represent distinct physical situations. The periodic condition assumes an infinite space where the maps repeat for each N maps. Mathematically, this condition is represented by:

$$x_n^{(i)} = x_n^{(i \pm N)} \tag{3}$$

Lyapunov spectrum represents one of the most important geometrical invariant of a dynamical system. The knowledge of this spectrum allows one to evaluate other invariants as the Kolmogorov-Sinai entropy. The analysis of Lyapunov spectrum in coupled maps can use the same methodology employed for a single map. Hence, let us assume coupled maps expressed by:

$$x_{n+1}^{(i)} = f(x_n^{(1)}, \dots, x_n^{(i)}, \dots, x_n^{(N)}) \tag{4}$$

The Lyapunov exponents determination needs to consider the variation of each cell under some perturbation in initial conditions, $x_0^{(i)}$. The Jacobian matrix is calculated to each iteration as follows (Shibata, 2001),

$$J_n = \begin{pmatrix} \frac{\partial x_{n+1}^{(1)}}{\partial x_n^{(1)}} & \frac{\partial x_{n+1}^{(1)}}{\partial x_n^{(2)}} & \dots & \frac{\partial x_{n+1}^{(1)}}{\partial x_n^{(N)}} \\ \frac{\partial x_{n+1}^{(2)}}{\partial x_n^{(1)}} & \frac{\partial x_{n+1}^{(2)}}{\partial x_n^{(2)}} & \dots & \frac{\partial x_{n+1}^{(2)}}{\partial x_n^{(N)}} \\ \vdots & \vdots & \ddots & \vdots \\ \frac{\partial x_{n+1}^{(N)}}{\partial x_n^{(1)}} & \frac{\partial x_{n+1}^{(N)}}{\partial x_n^{(2)}} & \dots & \frac{\partial x_{n+1}^{(N)}}{\partial x_n^{(N)}} \end{pmatrix} \tag{5}$$

Then, defining

$$R_n = \prod_{k=1}^n J_k \tag{6}$$

Lyapunov exponents, $\lambda^{(i)}$, are evaluated from the eigenvalue $\sigma^{(i)}$ of R_n , as follows (Holden & Zhang, 1992):

$$\lambda^{(i)} = \lim_{n \rightarrow \infty} \frac{1}{n} \ln |\sigma^{(i)}| \tag{7}$$

By considering the specific situation of coupled logistic maps where the coupling is defined by power law as presented in Eq.(1), the Jacobian matrix is written by:

$$[J_n]_{ij} = A_{ij} f'(x_n^{(j)}) \tag{8}$$

where A is a coupling dependent matrix (Batista & Viana, 2001):

$$A_{ij}(\varepsilon, \alpha) = \begin{cases} 1 - \varepsilon, & \text{if } i = j \\ \varepsilon |i - j|^{-\alpha} / \eta(\alpha), & \text{if } |i - j| \leq N' \\ \varepsilon (N' - |i - j|)^{-\alpha} / \eta(\alpha), & \text{if } |i - j| > N' \end{cases} \quad (9)$$

At this point, it is possible to use the classical algorithm due to Wolf *et al.* (1985) that uses the Gram-Schmidt orthonormalization of vectors of the tangent space (Lu *et al.*, 2005):

$$\mathbf{e}_1 = \frac{\mathbf{v}_1}{\|\mathbf{v}_1\|} \quad \mathbf{e}_2 = \frac{\mathbf{v}_2 - (\mathbf{v}_2 \cdot \mathbf{e}_1)\mathbf{e}_1}{\|\mathbf{v}_2 - (\mathbf{v}_2 \cdot \mathbf{e}_1)\mathbf{e}_1\|} \quad (10)$$

This approach allows the evaluation of the principal directions of the ellipsoid centered at a fiducial trajectory. The norms of the orthonormalized vectors at the denominator of $N_k^{(i)}$ are used to calculate the Lyapunov exponents. Therefore, after n iterations:

$$\lambda_n^{(i)} = \frac{1}{n} \sum_{k=1}^n \ln N_k^{(i)} \quad (11)$$

The Kolmogorov-Sinai entropy density is an index that can be calculated from the positive Lyapunov exponents as follows:

$$h = \frac{1}{N} \sum_{i=1}^{N, \lambda_i > 0} \lambda_i \quad (12)$$

Hence, when the entropy density vanishes there is no positive Lyapunov exponent and, therefore, there is no chaos. On the other hand, positive values of the entropy are related to chaos.

3. DYNAMICAL ANALYSIS

Numerical simulations are carried out by assuming a grid with $N = 21$ and non-homogeneous values of parameter β through the grid. In general, the grid is split in two parts and each one has different value of this parameters. Basically, we need to analyze the spatial interaction between two qualitative different behaviors. The left side is defined from $i = 1$ to $i = 11$ being related to parameter β_L , while the right side is defined from $i = 12$ to $i = 21$ being related to parameter β_R . Values of parameter β are chosen in order to consider different qualitative behaviors of the isolated map, that can be identified from a bifurcation diagram presented in Figure 2: 0 (period-1, stationary); 3.2 (period-2), 3.55 (period-8); 3.6, 3.7, 3.8 (chaotic); 3.835 (period-3 – periodic-window); 3.9, 4 (chaotic). All simulations are conducted assuming that parameter ε is between 0 and 1, while the parameter α is between 0 and 3. Periodic boundary conditions are focused on and different kinds of initial conditions are imposed to the system.

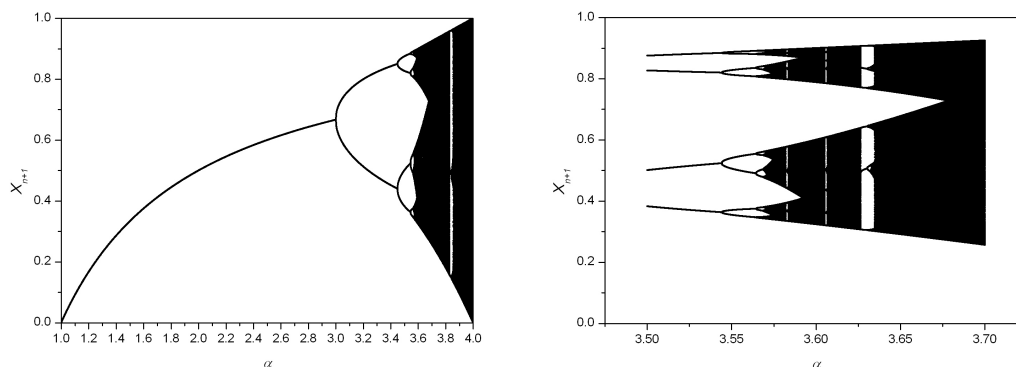


Figure 2. Logistic map bifurcation diagram.

Initially, let us consider an interaction between two dramatic behaviors: stationary ($\beta_L = 0$) and chaotic ($\beta_R = 4$). By assuming coupling parameters $\alpha = 3$ and $\varepsilon = 0.165$, the homogeneous grid with $\beta = 4$ presents a chaotic behavior with $h = 0.277$ over a period-2 dynamics. On the other hand, the dynamics with $\beta = 0$ is stationary. Figure 3 shows spatiotemporal response presented as an overlap of the last 30 iterations after 10,000. Two different initial conditions are of concern: $x_0^{(i)} = 0$, except for $x_0^{(1)} = 0.1$; $x_0^{(10)} = 0.1$, vanishing all others. Both situations are related to a chaotic response within a period-2 response which can be assured by the entropy density values $h = 0.0267$ (Figure 3a) and $h = 0.0245$ (Figure 3b). Note that the spatiotemporal aspects are altered by the initial conditions.

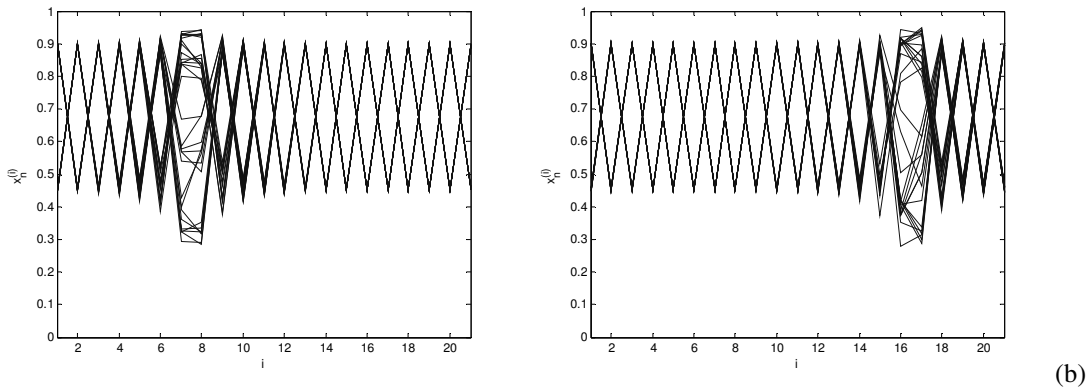


Figure 3. Overlap of the last 30 iterations after 10,000 for periodic boundary response with $\alpha = 3$ and $\varepsilon = 0.165$.

The non-homogeneous case is now focused on and the pattern of the homogeneous system is altered due to the influence of the left side response. Figure 4 presents the response of this non-homogeneous grid for different random initial conditions. Under this condition, the entropy density vanishes and the system presents a period-2 response that can be altered due to initial conditions. Figure 4 presents the system response for different initial conditions showing a period-4 together with the preponderant period-2 response.

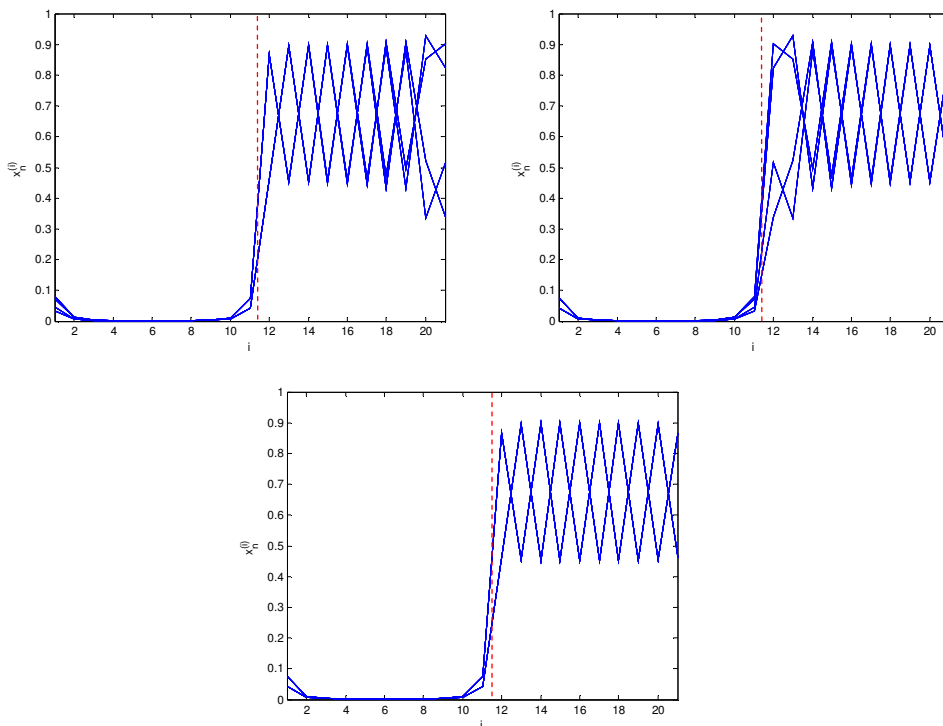


Figure 4. Overlap of the last 30 iterations after 10,000 for $\beta_L = 0$ and $\beta_R = 4$, $\alpha = 3$ and $\varepsilon = 0.165$ for three different random initial conditions.

If we consider a weak coupling among maps, represented by $\varepsilon = 0.08$, the grid presents a chaotic behavior ($h = 0.1297$) although strongly suppressed in the first half of the grid (Figure 5). Entropy shows an intermediate value between the values of each isolated half ($h = 0$ and $h = 0.4173$, respectively), showing that the resulting chaotic behavior is really damped by the maps where $\beta = 0$.

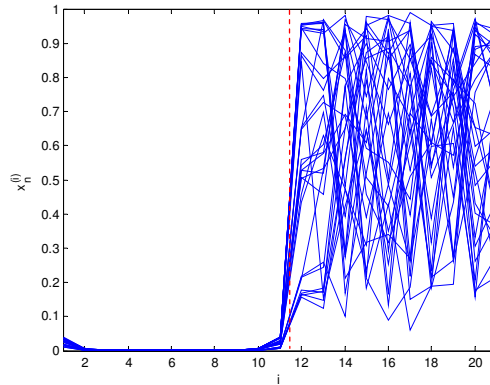


Figure 5. Overlap of the last 30 iterations after 10,000 for $\beta_L = 0$ and $\beta_R = 4$, $\alpha = 3$ and $\varepsilon = 0.08$. Random initial conditions.

A global analysis of the grid with $\beta_L = 0$ and $\beta_R = 4$ is done through the observation of the Kolmogorov-Sinai entropy density surface (Figure 6). When $\varepsilon = 0$, it is possible to observe that the entropy density has a value that is related to an average of Lyapunov exponents of the isolated maps, i.e., zero for the left side and 0.69 for the right side, that gives ~ 0.33 . The most important observation is done in the region with high values of both coupling parameters, where entropy density value of the non-homogeneous grid is positive for parameter combinations where the homogeneous grid with $\beta = 4$ results in entropy equal to zero. It can be concluded that the presence of maps with $\beta = 0$ does not allow the pattern selection and, as consequence, there is a chaos suppression when the grid assumes strong local coupling. A periodic valley can be observed around $\varepsilon = 0.05$ and low values of α , where the grid dynamic develops period-3 and period-6 behavior.

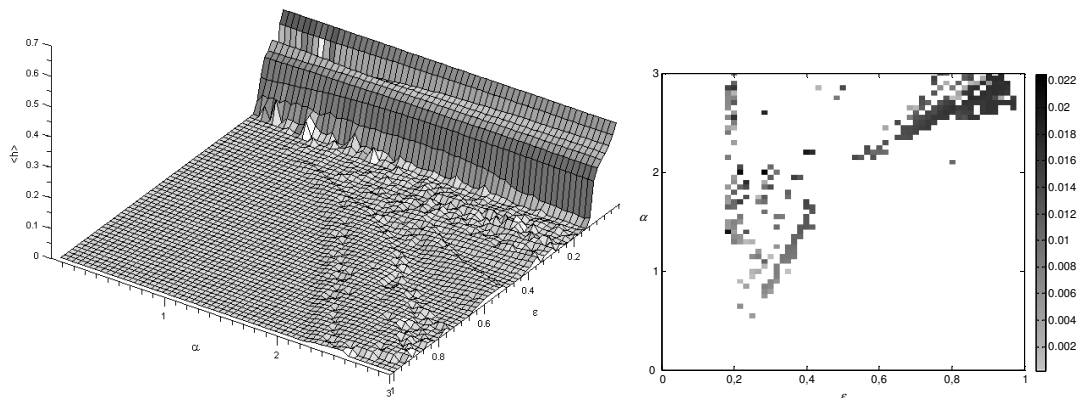


Figure 6. Entropy density surface for $\beta_L = 0$ and $\beta_R = 4$. On the right side, the regions where entropy of non-homogeneous grid is higher than the homogenous grid are highlighted.

When $\beta_L = 3.2$ (related to a period-2 behavior) and $\beta_R = 4$ (chaos), the grid develops chaotic behavior ($h = 0.0134$), although highly suppressed by the period-2 in the first half of the grid. This observation shows that when $\beta_L = 3.2$, although it is related to a periodic behavior if isolated, the whole grid has a chaotic pattern (Figure 7).

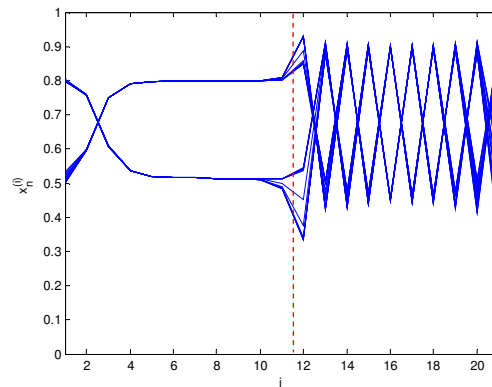


Figure 7. Overlap of the last 30 iterations after 10,000 for $\beta_L = 3.2$ and $\beta_R = 4$, $\alpha = 3$ and $\varepsilon = 0.165$. Random initial conditions.

The next scenario treated deals with $\beta_L = 0$ (stationary) and $\beta_R = 3.835$, that corresponds to a period-3 window in the bifurcation diagram of the isolated logistic map. It would be reasonable to say that a combination of two halves that develop periodic dynamics when isolated should also result in a periodic response for the coupled grid. As can be seen in Figure 8, a chaotic pattern is achieved under this condition ($h = 0.2057$), although the grid is composed only of maps that develop periodic motion when isolated. This observation differs from the previous, that the coupling restrains chaos development, by suppression of individual independence of each map.

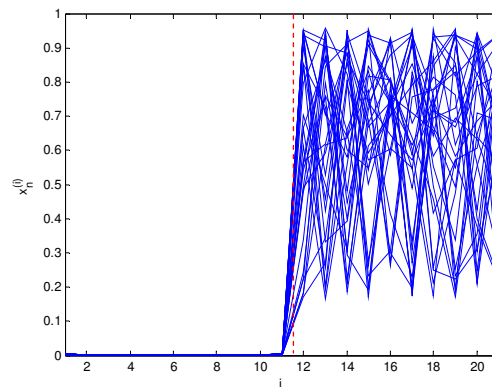


Figure 8. Overlap of the last 30 iterations after 10,000 for $\beta_L = 0$ and $\beta_R = 3.835$, $\alpha = 3$ and $\varepsilon = 0.01$. Random initial conditions.

At this point, a stronger coupling is assumed and the chaotic behavior is still occurring (Figure 9), but with a different spatial pattern. This is in accordance with the observed tendency that chaos is suppressed by strong coupling among the maps. The interface between grid halves shows a smoother change of pattern, typical of strong coupling.

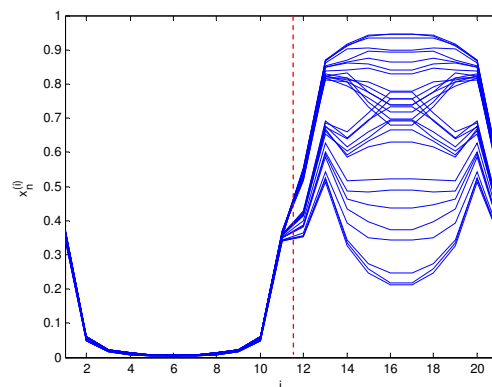


Figure 9. Overlap of the last 30 iterations after 10,000 for $\beta_L = 0$ and $\beta_R = 3.835$, $\alpha = 3$ and $\varepsilon = 0.8$. Random initial conditions.

At this point, two parameters corresponding to periodic response are of concern. Let us consider $\beta_L = 3.56$ (period-8 region), $\beta_R = 3.835$ (period-3, inside the periodic window), and coupling characteristic represented by $\alpha = 0.5$ and $\varepsilon = 0.1$. Under these assumptions, the system presents an entropy $h = 0.0927$ that could be understood as a chaos superposed to a period-2 response (Figure 10).

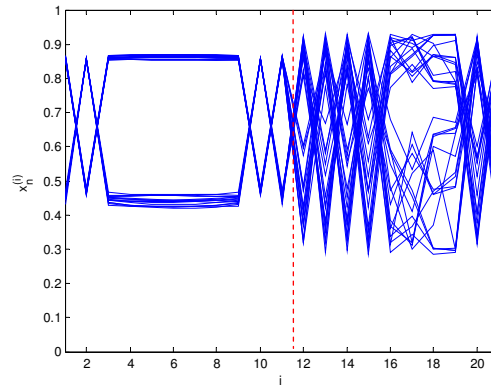


Figure 10. Overlap of the last 30 iterations after 10,000 for $\beta_L = 3.56$ and $\beta_R = 3.835$, $\alpha = 0.5$ and $\varepsilon = 0.1$. Random initial conditions.

By changing the coupling parameters for $\alpha = 3$ and $\varepsilon = 0.01$, the grid also develops chaotic response with entropy density $h = 0.2069$ (Figure 11). This result represents the chaos of the right side being spread to the left side.

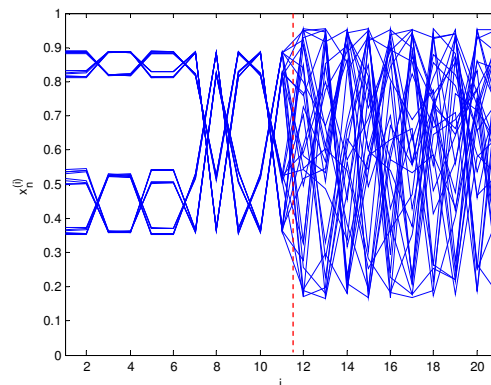


Figure 11. Overlap of the last 30 iterations after 10,000 for $\beta_L = 3.56$ and $\beta_R = 3.835$, $\alpha = 1$ and $\varepsilon = 0.01$. Random initial conditions.

Now the coupling is intensified ($\alpha = 3$ and $\varepsilon = 0.18$). This coupling in a homogeneous grid with $\beta = 4$ is associated with a period-4 response. For the non-homogeneous grid with $\beta_L = 3.56$ and $\beta_R = 3.835$ the resulting dynamic is chaotic ($h = 0.0112$) as can be seen in Figure 12. This result is interesting because the same parameter combination, if applied to homogeneous grid with $\beta = 4$, i.e., only maps that develops chaotic response when isolated, causes a periodic behavior and, if applied to non-homogenous grid with maps that develops periodic response when isolated, causes a chaotic behavior. This observation shows the unpredictability related to this kind of system. The interface between the halves follows the dynamic of each sector, with a chaotic modulation superposed in a period-2 response.

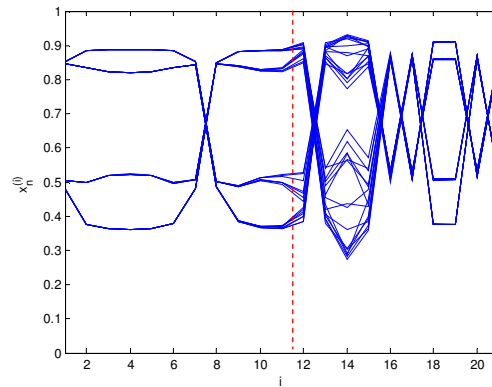


Figure 12. Overlap of the last 30 iterations after 10,000 for $\beta_L = 3.56$ and $\beta_R = 3.835$, $\alpha = 3$ and $\varepsilon = 0.18$. Random initial conditions.

A new situation is now focused on considering a grid with $\beta_L = 4$ (chaos) and $\beta_R = 3.5$ (period-4 response), $\alpha = 3$ and $\varepsilon = 0.2$. The homogeneous grid with $\beta = 3.5$ can present transient chaos depending on the initial conditions, but the steady state dynamics has a period-4 response. Therefore, we are combining two grids that, isolated, are related to periodic response. Figure 13 presents overlap of the last 30 iterations where it should be observed the spatiotemporal pattern is related to period-4 and period-2 responses. It is also noticeable in this pattern that the map eighteen develops a period-5 response and the interface between both halves presents period-12 response. This unpredictable combination of different periodic responses is suitable to describe the pattern creation capability of natural systems.

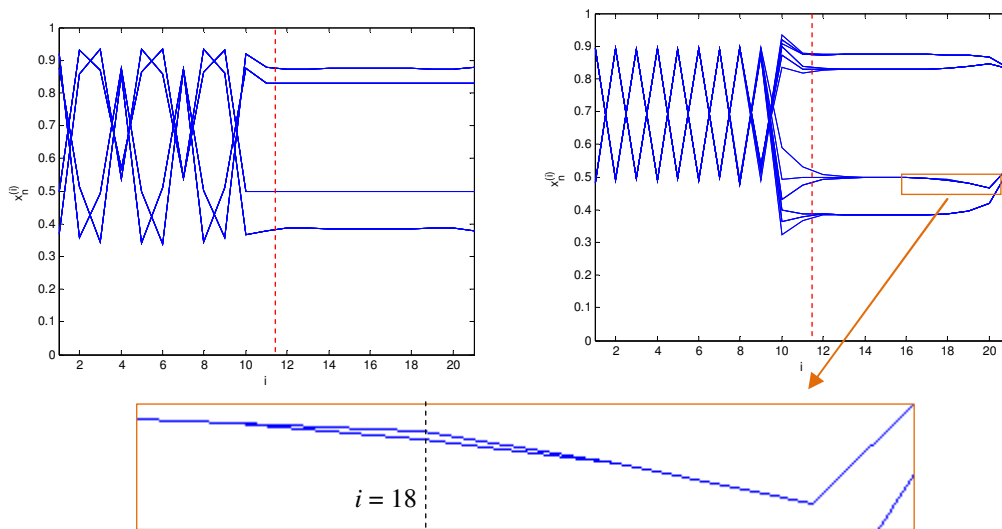


Figure 12. Overlap of the last 30 iterations after 10,000 for $\beta_L = 4$ and $\beta_R = 3.5$, $\alpha = 3$ and $\varepsilon = 0.2$ for two different random initial conditions. Detail of period-5 dynamics in map $i = 18$.

4. CONCLUSIONS

The spatiotemporal dynamics of coupled logistic map is of concern. Basically, we analyze the spatial interaction between two qualitative different behaviors. The grid is split in two parts evaluating how they interact. Periodic boundary condition is of concern. This kind of condition imposes greater homogeneity along the maps, since each side interact in both ends. In general, when there is a half with periodic response and the other with chaotic response, the global response tends to suppress chaos. If one half is related to a periodic window ($\beta = 3.835$) the interaction between both parts inhibits the period-3 response, resulting in a chaotic pattern. It is also possible to obtain unexpected period-12 response in the interface between parts. In general, this work shows different kinds of patterns that could emerge from spatiotemporal nonlinear interactions.

5. ACKNOWLEDGEMENTS

The authors acknowledge the support of Brazilian Research Councils CNPq and FAPERJ.

6. REFERENCES

- Awrejcewicz, J., 1991, "Nonlinear dynamics of a two-body nonlinear mechanical system", *Computer Methods in Applied Mechanics and Engineering*, 91, pp. 1093-1108.
- Batista, A.M., Viana, R.L., 2001, "Lyapunov exponents of a lattice of chaotic maps with a power-law coupling", *Physics Letters A*, 286, pp.134-140.
- Holden, A.V., Zhang, H., 1992, "Lyapunov exponent spectrum for a generalized coupled map lattice", *Chaos, Solitons & Fractals*, 2, pp.155-164.
- Kaneko, K., 1990, "Supertransients, spatiotemporal intermittency and stability of fully developed spatiotemporal chaos", *Physics Letters A*, 149, pp. 105-112.
- Kaneko, K., 1992, "Theory and applications of coupled map lattices", John Wiley & Sons.
- Lai, Y.C., Grebogi, C., 1999, "Modeling of coupled chaotic oscillators", *Physical Review Letters*, 82, pp. 4803-4806.
- Lu, J., Yang, G., Oh, H., Luo, A.C.J., 2005, "Computing Lyapunov exponents of continuous dynamical systems: Method of Lyapunov vectors", *Chaos, Solitons & Fractals*, 23, pp. 1879-1892.
- May, R.M., 1976, "Simple mathematical models with very complicated dynamics", *Nature*, 261, pp. 459-467.
- Savi, M.A., 2007, "Effects of randomness on chaos and order of coupled logistic maps", *Physics Letters A*, 364, 5, pp.389-395.
- Shibata, H., 1998, "Quantitative characterization of spatiotemporal patterns", *Physica A*, 253, pp. 134-142.
- Shibata, H., 1998, "Quantitative characterization of spatiotemporal chaos", *Physica A*, 253, pp. 428-449.
- Shibata, H., 2001, "KS entropy and mean Lyapunov exponent for coupled map lattices", *Physica A*, 292, pp. 182-192.
- Umberger, D.K., Grebogi, C., Ott, E., Afeyan, B., 1989, "Spatiotemporal dynamics in a dispersively coupled chain of nonlinear oscillators", *Physical Review A*, 39, pp.4835- 4842.
- Vasconcelos, D.B., Viana, R.L., Lopes, S.R., Batista, A.M., Pinto, S.E. de S., 2004, "Spatial correlations and synchronization in coupled map lattices with long-range interactions", *Physica A*, 343, pp. 201-218.
- Viana, R.L., Grebogi, C., Pinto, S.E. de S., Lopes, S.R., Batista, A.M., Kurths, J., 2005, "Bubbling bifurcation: Loss of synchronization and shadowing breakdown in complex systems", *Physica D*, 206, pp. 94-108.
- Waldrop, M.M., 1992, "Complexity", Simon & Schuster Paperbacks.
- Willeboordse, F., 1992, "Selection of windows, attractors and self-similar patterns in a coupled map lattice", *Chaos, Solitons & Fractals*, 2, 6, pp. 609-634.
- Wolf, A., Swift, J. B., Swinney, H. L. & Vastano, J. A., 1985, "Determining Lyapunov Exponents from a Time Series", *Physica 16D*, pp.285-317.

7. RESPONSIBILITY NOTICE

The authors are the only responsible for the printed material included in this paper.